academicJournals

Vol. 12(3), pp. 24-41, 15 February, 2017
DOI: 10.5897/SRE2016.6459
Article Number: A241D8463605
ISSN 1992-2248

http://www.academicjournals.org/SRE

Scientific Research and Essays

Full Length Research Paper

Groundwater resilience to climate change in the Eastern Dead Sea Basin – Jordan

Marwan Alraggad[1]*, Bart Johnsen-Harris[2], Ahmad Shdaifat[1], Moh`d Kotaiba Abugazleh[3] and Arwa Hamaideh[1]

[1]Water, Environment and Energy Center, University of Jordan, Jordan.
[2]Masar Center, Amman, Jordan.
[3]University of Jordan, Jordan.

Received 28 September, 2016; Accepted 2 November, 2016

Pumping of 82 MCM/yr from Mujib Basin (Eastern Dead Sea), coupled with the 54 MCM/yr recharge rate, has led to diminished groundwater levels and dramatically affects ecosystem services. Climate change compounds these issues by reducing recharge and increasing the ecosystem's hydrological demand. This paper investigates groundwater resilience to climatic changes in Mujib Basin by modeling resilience for the years 2014 and 2050. Resilience of groundwater was modeled to long term changes as "low" in the central parts of the study area due to low saturated thickness and high pumping rates. Resilience was modeled as "high" to "very high" in areas with high saturated thickness and higher replenishment rates. Water budget components were modeled through the J2000 hydrological model, giving a groundwater recharge of 54 MCM/yr. Statistical downscaling of global circulation models indicated a 21% decline in precipitation by the year 2080 with 2 and 3° increases in maximum and minimum temperature respectively. Recharge for the year 2050 was recalculated based on the downscaling and prediction results to be 30% less than current recharge. Continuous over-pumping with recharge reduction will cause a 30-70% reduction in saturated thickness by the same year. Modeling groundwater resilience under the new conditions showed a severe impact on the study area especially the central parts which are expected to comprise a semi dry aquifer by 2050.

Key words: Jordan, Dead Sea, groundwater resilience, climate change.

INTRODUCTION

Jordan is characterized by a semi-arid climate where groundwater is the primary source of fresh water. Groundwater serves as more than 65% of the total water supply, which is around 900 MCM/yr (MWI, 2013). Available water resources, especially groundwater resources, have been subjected to increasing pressures over the last three decades in order to satisfy the needs of Jordan's rapid population growth. Additionally, climate variability has disturbed the recharge rates of different aquifers due to increasing evaporation rates and decreasing precipitation.

The Dead Sea Basin is a vital source of groundwater in

*Corresponding author. E-mail: mar_raggad@yahoo.com.

the country as a result of its high productivity, supplying about 8% of the total water supply. The basin hosts the lowest-altitude natural reserve in the world, known as Mujib reserve, at 420 m.b.s.l. located in the western parts of the basin. Annual groundwater pumping from this basin was about 79 MCM in 2013 with a recharge rate of 57 MCM/yr (MWI, 2014).

Groundwater development in the Dead Sea Basin began in the early '70s to cover local water needs. This development expanded to transboundary water pumping in the '90s with more than 150 wells drilled in the upper cretaceous limestone aquifer-known locally as B2A7 (Salameh, 1996). Over-exploitation of the B2A7 aquifer system has resulted in a rapid plunge of the water table to more than 3.5 m in some areas, which affects wells' productivity, spring discharge, and related ecosystem services (USGS, 2013).

Climatic trends within the Dead Sea Basin are following the same trends as other basins in Jordan. Records from 1970–2010 showed a notable increase in temperature and a decline in precipitation rates, with a shift in the rainy season affecting aquifer replenishment rates (Abu-Allaban et al., 2015).

Measurements from the 1980s reported the basin's water quality as "good" to "fair" with total dissolved solids (TDS) of 300–800 mg/l (USGS, 2013). More recent TDS measurements show more than 1500 mg/l in the eastern regions of the study area, reaching more than 2100 mg/l in some water sources. In general, the basin's salinity is low in the vicinity of the recharge areas; salinity increases along the flow path towards the endpoints of discharge (Alraggad, 2009).

Thus, groundwater system in the area as a whole is being degraded dramatically. This urges the need to adopt new management tools. This study aims to shed the light on spatial variability of groundwater resilience to climatic conditions and man-made activities in order to develop an integrated groundwater management system.

METHODOLOGY

Study area

The Dead Sea Groundwater Basin (Figure 1) is located in the western part of Jordan near the borders with a total area of 6873.5 km^2.

The high topographic relief of the basin is a result of the Dead Sea transform fault system. This gives a contour variation ranging from 1200 m.a.s.l. in the southern parts of the area to a minimum of 420 m.b.s.l. near the Dead Sea (El-Naser et al., 1998). The basin displays a diverse array of land cover and use; according to the National Soil Map and Land Use project for Jordan, bare rocks are the dominant land cover, covering 62% of the basin (MWI, 1995). The rest of the basin's cover is composed of rain-fed vegetables and cereals, rain-fed fruit trees, and irrigated vegetables and trees. Land use is controlled by precipitation rates in addition to topography and other factors (MOA, 1993).

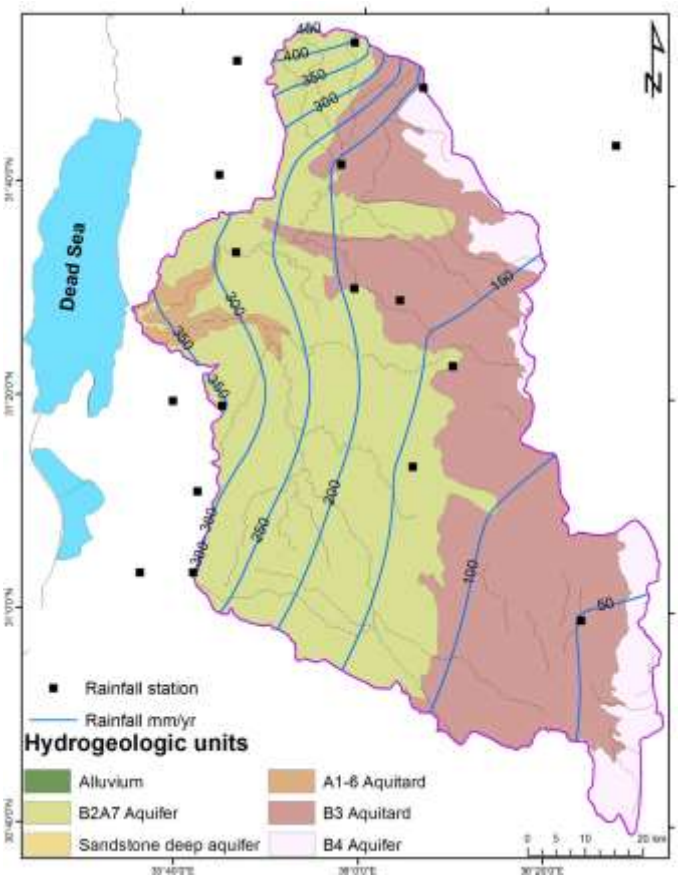

Figure 1. Mujib Basin with hydrogeologic units and yearly precipitation.

Water resources

All surface water in the basin runs toward the Dead Sea in the form of perennial or ephemeral systems, as the Dead Sea is a base topographic point (NWMP, 1977). The study area is well-sculptured due to the geological weathering activities occurring since the formation of the Dead Sea system (Alraggad, 2009).

Mujib Basin discharges into the Dead Sea through two main Wadis-Mujib and Wala-with a base flow sustained by local springs on the escarpment to the Dead Sea of 35 MCM and an annual flood flow of 65 MCM. Flood water is being generated after intense storms occurring in the wet season, extending from October to April.

The high topographical gradient towards the Dead Sea, with a prevailing wind direction facing the slope, allow for the occurrence of sudden cloud uplift resulting in an average precipitation range of less than 100 mm/yr in the Dead Sea area to more than 500 mm/yr in the eastern highlands (Abu Gazleh, 2014).

Due to relatively high precipitation rates in the north,

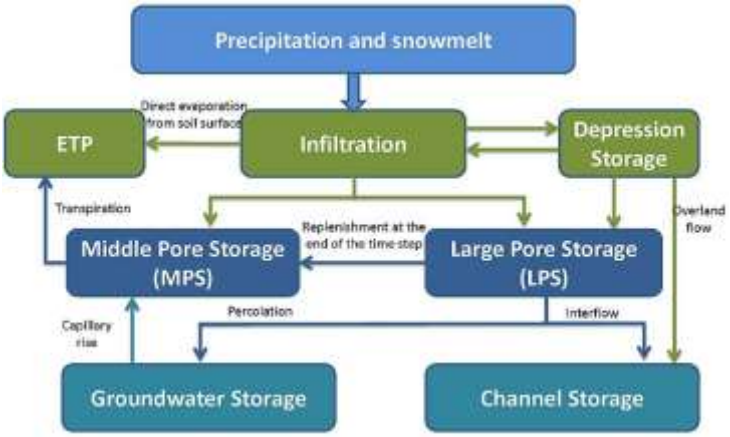

Figure 2. Concept of the J2000 model for water balance calculation (Krause, 2002).

groundwater flow is initiated. The groundwater flow regime in the B2A7 aquifer follows the topographic variation, with dominant flow direction from north to south and then follows the natural topographic slope towards the Dead Sea (BGR and WAJ, 1996; Alraggad, 2009).

Upon review of the IPCC Fourth Assessment Report climate model, projections show a consistent pattern of continuous warming of the climate in the Middle East with a less consistent pattern for precipitation (Solomon et al., 2007). The elevated minimum and maximum temperatures will enhance evapotranspiration and likely increase the intensity and variability of precipitation events. Impacts on groundwater are expected to be high considering that recharge is influenced by a series of processes such as evaporation, runoff, and soil saturation. This continuous warming will consume most of the precipitation by evapotranspiration and consequently groundwater recharge rate is the most affected component.

Groundwater recharge modeling

Several factors are affecting the recharge in the study area, including precipitation, topography, and soil cover. Site-specific field studies of recharge (infiltration measurements, lysimeters, etc.) are lacking, so, the J2000 water balance model was used for recharge calculation. The J2000 model, which is based on a water budget approach (Healy, 2010), has been applied to estimate recharge rate D (mm/year) distribution over the study area according to the following equation:

$$D = P - ET - \Delta S - R_{off} \quad (1)$$

where P is precipitation (mm/yr), ET is evapotranspiration (mm/yr), ΔS is the change in soil water storage in the soil column (mm/yr), and R_{off} is runoff (mm/yr).

The J2000 hydrological model provides physical-based modeling for water budget components for macro catchment areas (Krause and Kralisch, 2005). Within the J2000 system, simulation of hydrological processes is carried out in an environment where parameters of water balance are independent of each other. They are calculated separately, then simulated to calculate recharge (Schulz, 2013). Figure 2 provides the concept and general layout of the J2000 water balance system.

Precipitation

Weighted average method (Thiessen polygons) was used in order to build precipitation isohyets and to achieve adequate statistical certainty; data set for the time period (1970 – 2010) was obtained from MWI climate and rain stations with daily measurements. Daily records were analyzed in terms of basic statistics.

IDW method (Inverse Distance Method) was used to interpolate the data from precipitation long-term records, accompanied with elevation corrections to produce the isohyetal map. The resulting average precipitation was 220 mm/year in the central parts of the study area (Figure 1).

Evapotranspiration

The evapotranspiration within the study area was calculated to be high in the northern parts as a result of low relative humidity and presence of green cover,, while in the Dead Sea area where temperature is higher, the evapotranspiration is low due to high relative humidity which exceeds 90% with a scarce green cover. Climatic data are available on a daily basis from 4 stations within the study area and 3 stations around the basin's borders.

Evapotranspiration can be calculated using the J2000 ETP module based on the Penman-Monteith equation (1948). This method combined the energy balance with the mass transfer method. This combination was developed by scientists to be valid for green cover by adding more resistance factors (FAO, 1998). The resulted equation shown below represents the code of the ETP module in the J2000 model.

$$ETP_d = \frac{1}{L_d} \cdot \frac{s_d \cdot (R_{N_d} - G_d) + \rho \cdot c_P \cdot \frac{e_{s_d} - e_d}{r_a}}{s_d + \gamma_d \cdot \left(1 + \frac{r_{s_d}}{r_a}\right)} \cdot \left(\frac{S_0}{24}\right)$$

$$ETP_n = \frac{1}{L_n} \cdot \frac{s_n \cdot (R_{N_n} - G_n) + \rho \cdot c_P \cdot \frac{e_{s_n} - e_n}{r_a}}{s_n + \gamma_n \cdot \left(1 + \frac{r_{s_n}}{r_a}\right)} \cdot \left(1 - \frac{S_0}{24}\right)$$

Where:
$L_{d,n}$ ... latent heat of evaporation [Wm^{-2}] per [mmd^{-1}]
$s_{d,n}$ ... slope of the vapor pressure curve [$hPaK^{-1}$]
$R_{N\,d,n}$ ... net radiation [Wm^{-2}]
$G_{d,n}$ ... soil heat flux [Wm^{-2}]
ρ ... density of the air [kgm^{-3}]
c_p ... specific heat capacity of the air for constant pressure [$Jkg^{-1}K^{-1}$]
$e_{sd,n}$ ... saturation vapor pressure [hPa]
$e_{d,n}$ ... vapor pressure [hPa]
r_a ... aerodynamic resistance of the land cover [sm^{-1}]
$\gamma_{d,n}$ ... psychrometer constant [$hPaK^{-1}$]
$r_{sd,n}$ ... surface resistance of the land cover [sm^{-1}]
S_0 ... astronomic possible sunshine duration [h]

Data for time 1970–2010 were input in order to calculate evapotranspiration over the hydrological year extending from October to May. We found that the value of evapotranspiration was about 79% of the total precipitation.

The evapotranspiration model shown in Figure 3 indicates the high evaporation rates on the western highlands due to high wind speed and a large presence of green cover. Due to the topographic elevation, this area recorded a wind speed up to 3.9 m/s coupled with low relative humidity (around 65%) (MWI open files) which increases the evapotranspiration up to about 240 mm per wet season. Green cover exists in the form of rain-fed field crops and has helped in increasing transpiration during the growing season from October to June.

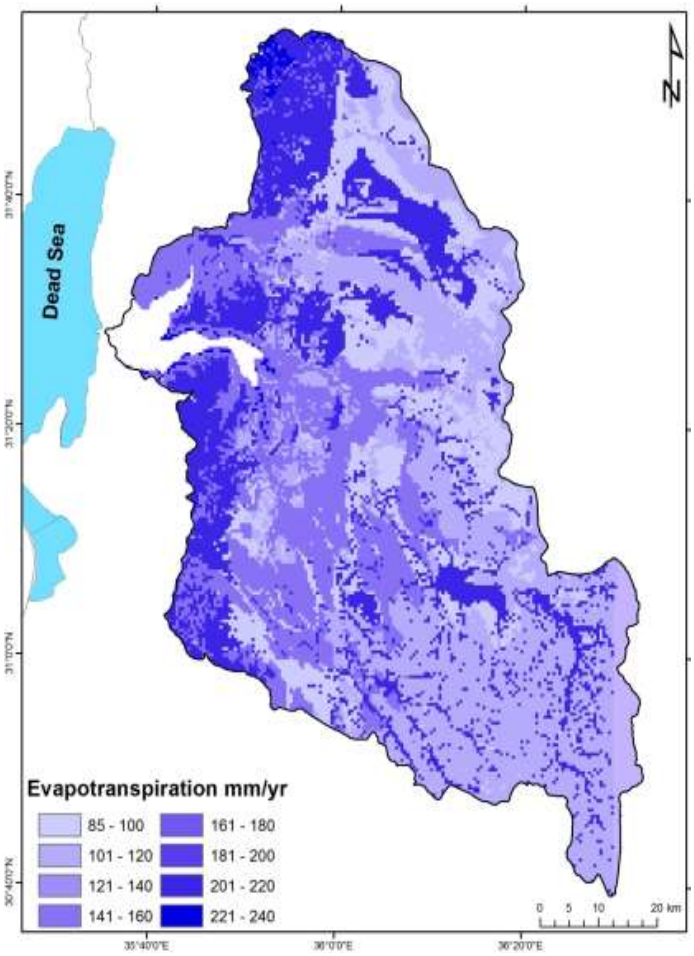

Figure 3. Evapotranspiration over the study area mm/yr.

Change in soil water storage

Soil in Jordan plays a significant role in the recharge process (MOA, 1995a), but has unfortunately not been widely studied in terms of hydraulic parameters. The groundwater system receives its input from the unsaturated soil zones, which differ in thickness and hydraulic properties. The recharge process can only start after the soil column is saturated.

Using the J2000 hydrological model, soil water storage was calculated as this model is a software framework used widely with GIS to investigate water budget (Kralisch et al., 2007). The start point of the J2000 model is the maximum infiltration rate functions. As this onset is crossed, the surplus water takes two paths; to be delivered to the groundwater system or to be stored in depressions such as drainage ditches.

One advantage of the J2000 model is that hydrological processes are simulated in the form of compressed units which are independent of each other. This allows the modification of the input data without the need for restructuring the whole model (Figure 3). Additionally, this model allows us to calculate any single parameter from the water budget (Krause, 2002); the change in soil water storage was calculated by using the soil model. The data needed for this module are the soil's physical and hydraulic parameters shown in Table 1.

The soil module of the J2000 for all soil units and types is represented by the soil pore volume which can be classified as follows (Scheffer and Schachtschabel, 1984):

Table 1. Soil based data for soil module in J2000.

Parameter	Description
SID	Soil type ID
depth	Soil depth
kf_min	Minimum permeability coefficient
depth_min	Depth of the horizon above the horizon with the smallest permeability coefficient
kf_max	Maximum permeability coefficient

i) Fine pores water storage (< 0.2 µm diameter) with high adsorption minimizing water movement within the soil profile.
Medium pores water storage (diameter 0.2 to 50 µm) which holds water against gravity due to its high adsorption. Water here can be extracted using suction potential.
ii) Coarse and macro pores water storage (> 50 µm diameter which stays in the soil for only 1 or 2 days, then gets driven by gravity to lower profiles or to the groundwater) (Scheffer and Schachtschabel, 1984).
iii) Fine pores water storage was ignored in the J2000 model as it is not available for hydrological processes due to the soil's high adsorption power.

Within the J2000 data input, the middle pores water storage corresponds to middle pore storage volume (MPS), which can only be emptied through evapotranspiration. Coarse and macro pores water storage corresponds to the volume of the large and macro pores (LPS), which is the source for groundwater recharge and channel storage.

As soil data are very limited within Mujib Basin; soil samples were collected by a soil core of 10 cm radius and 30 cm height samplers for laboratory testing. Samples from 50 referenced sites were collected during certain days after major rainy events in the rainy season. Collected samples represents the upper most 30, these samples were considered as a base to measure the overall soil water storage in the whole soil profile in the sampling sites. Soil profiles thicknesses were obtained from Ministry of Agriculture (MOA, 1995b).

All samples were tested at the department of applied geology at the University of Jordan to measure the kf_min, depth_min and kf_max, while the soil depths were recorded in the field.

Soil type ID parameters were recorded based on the analysis done for the soil samples, which in turn led to our categorization of all soils within the study area in classes based on infiltration capacity. These categories included classes ranging from class "Soil type A" with the highest infiltration capacity to class "Soil type D" with the lowest infiltration capacity. After the arrival of the analyzed data and parameters; the soil module of the J2000 was generated resulting with a 14.2 mm/year calculated average water storage in the soil.

Runoff

Runoff Curve Number method (Hjelmfelt, 1991; SCS, 1985, 2004) was used to calculate the runoff by using data from five gauging stations for more than 146 runoff records. Upstream gauging stations provided precipitation records for the period of 1970–2010; these records were plotted against the generated runoff recorded at the gauging station (Figure 4), giving an average runoff coefficient of 6.7% of the total rain.

Comparing the simulated to the measured runoff resulted in a good fit (Figure 5), with total runoff of 82.6 MCM for flood flow and 32.2 MCM for base. For the validation process; observed and simulated runoff values were interpreted as shown in in Figure 6, which indicates a good match among the two variables with $R^2 = 0.98$.

Recharge calculation

To calculate the recharge, GIS maps of the budget equation components (Equation 1) were recalculated and updated to J2000 model environment (based on water Equation 1). Results showed that the recharge over the study area (Figure 4) is distributed through zones reflecting the amount of recharge in each zone. The maximum recharge can be found in western parts of the study area with a value of about 54 mm/yr, while the lowest value can reach 1 mm/yr in the eastern part with almost zero recharge through the confining unit.

The final calculated water budget is shown in Table 2, where evaporation comprises 79% of the total rain with 4.7% limited recharge which corresponds to the range of previous calculations done by Khadeer (1997) and MWI (1993) with 3.5, 6.1 and 5.2% recharge respectively.

Groundwater resilience

Gunderson (2000) defined ecosystem resilience as "the amount of disturbance that an ecosystem could withstand without changing self-organized processes and structures.

The term "resilience" encompasses two main aspects of an ecosystem: ability to resist long term damage and recovery time following a disturbance (Gunderson, 2000).

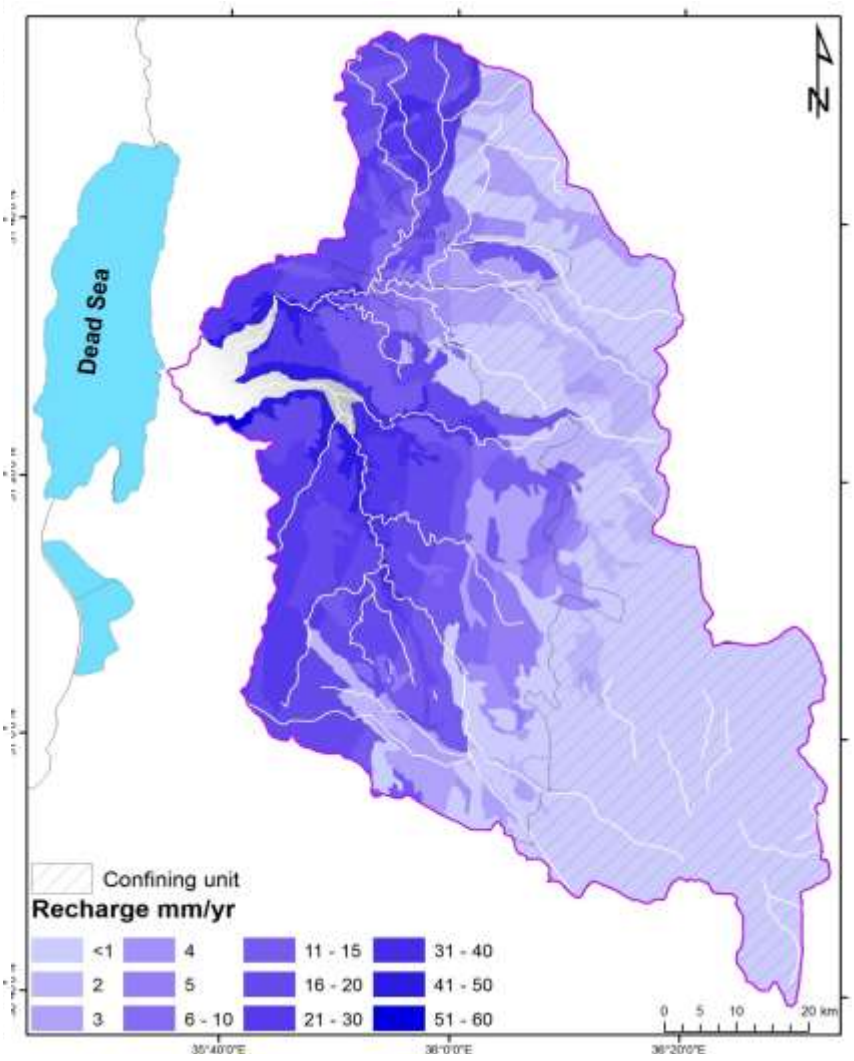

Figure 4. Modeled recharge over the study area mm/yr.

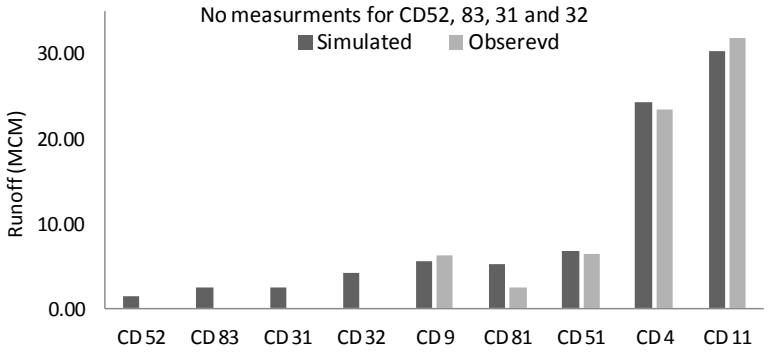

Figure 5. Simulated and observed runoff volumes for Mujib subcatchments.

As groundwater is considered an ecosystem, the Groundwater resilience to long term climatic shifts and general climate variability is determined by available groundwater storage. Since resilience increases with more aquifer storativity, large groundwater systems will be less affected by such stresses than smaller bodies. The whole concept of groundwater resilience relies on its physical and hydrogeological parameters.

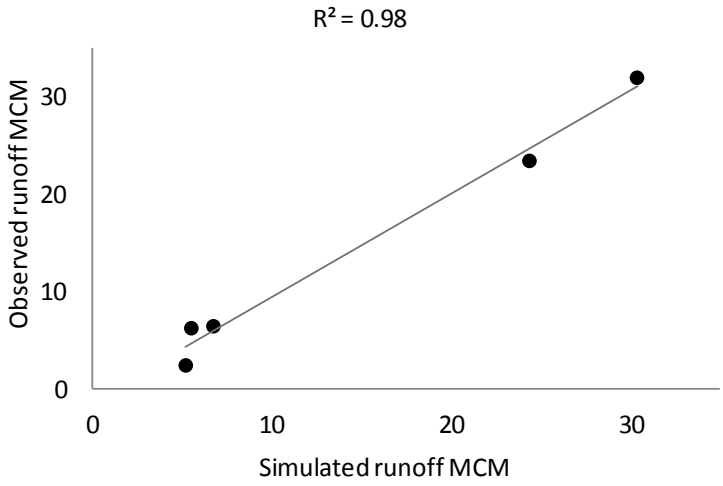

Figure 6. Correlation of observed and simulated runoff.

Table 2. Water balance from Mujib Basin.

Parameter	MCM	%
Precipitation	1148.6	
Evapotranspiration	902.5	78.6
Flood flow	82.6	7.19
Base flow	32.2	2.8
Soil storage	76.5	6.65
Recharge	54.8	4.76

Occurrence of groundwater is controlled by key factors such as geology, geomorphology, topography, and precipitation in the current and past times. The interaction of these factors gives hydrogeological system diverse complexities with countless variations in groundwater quality and quantity (MacDonald et al., 2011).

MacDonald et al. (2011) developed a GIS thematic mapping procedure to evaluate aquifer resilience based on spatial distribution of groundwater storage, aquifer permeability, and the annual rate of recharge. The model's input is based on characterizing aquifer hydraulics such as permeability and transmissivity, effective porosity of the vadose and saturated zones, saturated thickness, and groundwater recharge.

Simsek (2007) developed a modification to the DRASTIC groundwater vulnerability index by Aller et al. (1987) shown in Table 3. This model uses hydraulic parameters of the aquifer such as transmissivity and specific capacity as the main model constituents, with additional consideration of renewability rates in terms of recharge, aquifer lithology, and water table.

$$\text{API (Aquifer Potential Index)} = TwxTr + SwxSr + RwxRr + LwxLr + DwxDr\ldots\ldots \quad (2)$$

where: Tw: Transmissivity weighting value
Tr: Coefficient of transmissivity rating value
Sw: Specific capacity weighting value
Sr: Coefficient of specific capacity rating value
Rw: Recharge weighting value
Rr: Coefficient of recharge rating value
Lw: Aquifer lithology weighting value
Lr: Coefficient of aquifer lithology rating value
Dw: Depth to water table weighting value
Dr: Coefficient of the water table rating.

Both studies neglected the effect of groundwater pumping (P) on the aquifer resilience, but, in this study it was added to the previous equation as $P_W \times P_R$.

Data on transmissivity from 94 wells were obtained with good areal coverage in most parts of the basin. The exception was the southeastern parts, where we interpolated transmissivity using the IDW method from 14 wells located 20 km south of the basin within the same aquifer unit of the limestone.

Values for transmissivity were derived from the following equation:

$$T=K\times b$$

Table 3. Groundwater resilience parameters.

Criteria	Weight	Classes	Rate
Transmissivity (m^2/day)	5	>500	5
		400 – 500	4
		300 – 399	3
		200 – 299	2
		< 200	1
Specific capacity (m^2/day)	4	>500	5
		300 – 500	4
		100 – 299	3
		50 – 99	2
		< 50	1
Groundwater recharge (mm/yr)	3	50 – 60	5
		40 – 49	4
		30 – 39	3
		20 – 29	2
		< 20	1
Aquifer lithology	2	Karst. Limestone	3
		Limestone	2
		Marl limestone	1
Depth to water (m)	1	<50	5
		50 – 99	4
		100 – 199	3
		200 – 299	2
		>300	1
Abstraction (1000m^3/yr)	3	<25	4
		25 – 99	3
		100 – 300	2
		>300	1

Modified after Simsek (2007).

T: Transmissivity, K: Hydraulic conductivity and b: Aquifer saturated thickness.

Permeability values from MWI (1970), Alraggad (2009) and MWI Open Files (2013) were recorded to be in the range of 1.4×0^{-5} to 2.2×10^{-4} m/s which applies to the karstified lime stone aquifer.

The spatial distribution of permeability values showed a high correlation to main geologic structures resultant of the Dead Sea transform fault (BGR and MWI, 2005; Alraggad, 2009). The central highlands of the study area recorded the highest structural complexity, combined with permeability up to 2.2×10^{-4} m/s.

The structural contour map of the Aquifer Base (BGR and WAJ, 1995) was used in the simulation of saturated thickness in the Arc groundwater tool by Esri (2010). We analyzed data from 23 observation wells tapping the limestone aquifer to generate the groundwater table map. The map indicated a high groundwater table around 1000 m.a.s.l. in the highlands to less than 400 m.a.s.l. in the lowlands.

Aquifer saturated thickness was calculated as the difference between the free water table and the aquifer base, which ranged from 20 m up to 250 m.

Finally, transmissivity was measured in the ArcMap raster calculator to be in the range of 3 to 986 m^2/day as shown in Figure 7a.

Specific capacity can be obtained from the yield of boreholes divided by the total drawdown during a long-duration pumping test (Kruseman and de Ridder,1991). Records of well tests are available at the MWI data bank2014 for more than 370 groundwater wells in the area. Specific capacity based on these records was calculated to be in the range of 1 to 60 m (Figure 7b).

Recharge rate is adopted from this work as estimated

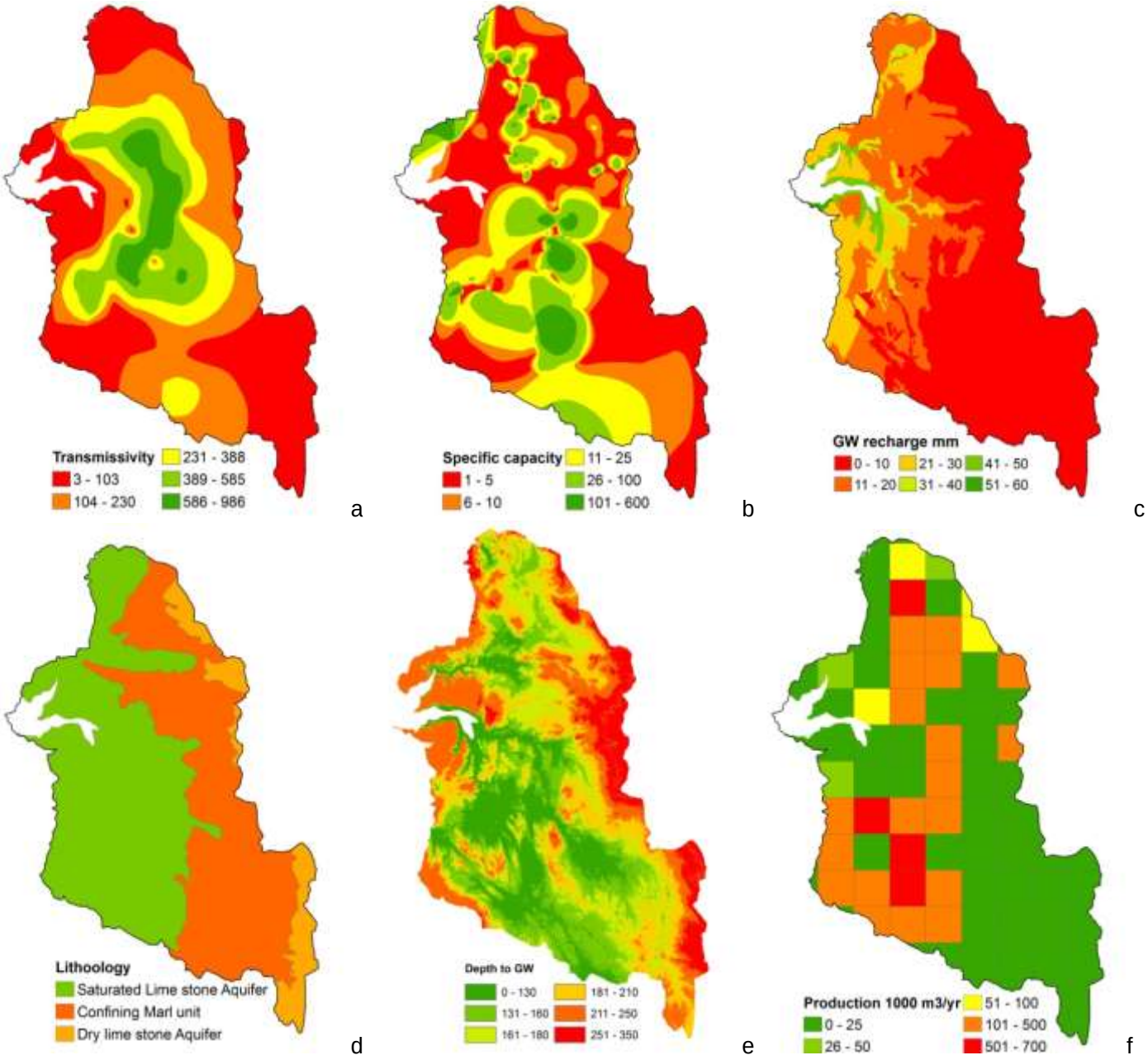

Figure 7. Calculated resilience parameters.

to be >1 to 60 mm/yr, while aquifer lithology was obtained from Margane et al. (2002) where, limestone aquifer outcrops on more than 50% of the total basin area with a confining bituminous Marl and Marly limestone beds along the eastern parts of the basin (Figure 7c).

Depth to groundwater table was calculated by the ArcMap raster calculator defined as the difference between the surface altitude and the groundwater table altitude, and it ranged from 40 to 400 m (Figure 7e).

Monthly groundwater pumping, which counters the natural recharge, takes place through more than 350 wells pumping about 79 MCM/yr (MWI, 2013). Monthly production data were accumulated on a yearly basis and related to 10 × 10 km area (pixels). Joining the pixel file with yearly production allowed us to define total yearly pumping rate from each pixel containing production wells. The active pumping pixels showed a high variability from >25000 to 980000 m^3/yr, where high values represent major well fields in the basin (Figure 7f).

Based on the combination of the previous thematic maps, the area showed different cumulative resilience ranks (Figure 8). The area was classified into 4 main

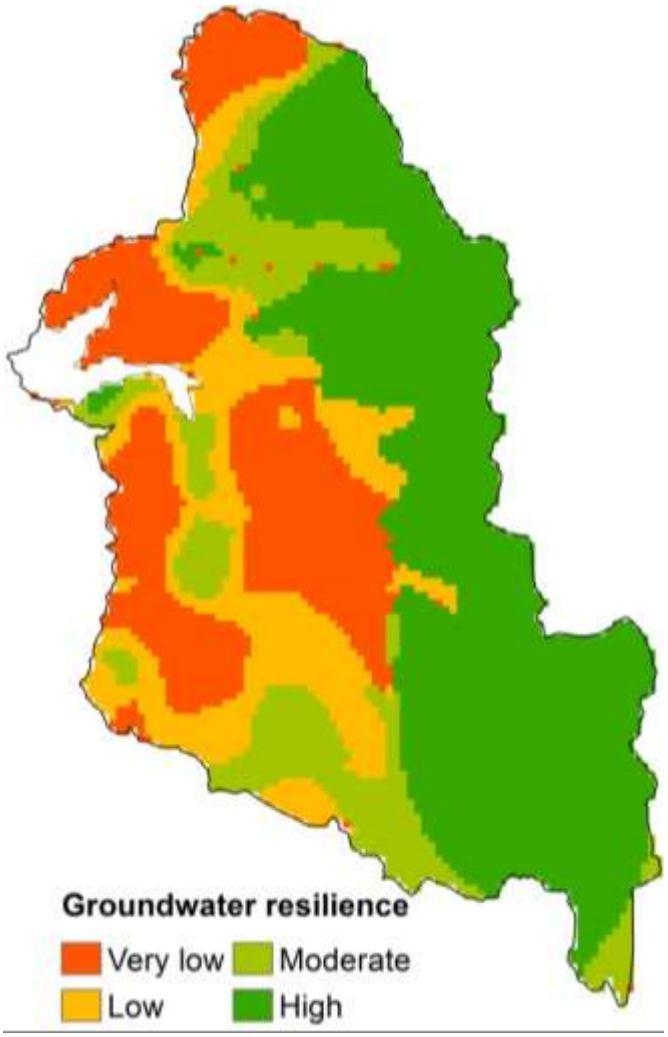

Figure 8. Groundwater resilience map.

classes as “very low,” “low,” “moderate,” and “high.” Eastern parts of the basin were modeled to have the highest resilience due to high saturated thickness, transmissivity, and specific capacity which overcomes the low recharge rates. Due to high pumping rates, low transmissivity, and moderate groundwater recharge in the central parts, we marked the area as very low resilience with an expected high impact from climate change.

The western and northern mountains showed a very low resilience-even with the relatively high recharge rate-due to limited saturated thickness and transmissivity.

The previous model implied that transmissivity, which is based on the saturated thickness, is the key player in groundwater resilience.

The resulting resilience map draws a major concern of high well pumping in a low resilience area, amplifying the effects of climate change.

Saturated thickness in this area is less than 70 m, with limited recharge of 8 to 13 mm/yr and a high variability of precipitation, adding more pressures on the system. The impact of groundwater recharge can be maximized through its impact on water level and the saturated thickness. Reduction of future recharge due to elevated temperature and lowered precipitation will reduce the saturated thickness, transmissivity, and depth to groundwater.

In order to model the effects of climatic variability on groundwater resilience, climate modeling is necessary in order to measure predicted future climatic conditions which will be used as an input to resilience analysis. This can be accomplished by predicting groundwater recharge and saturated thickness under specified climatic conditions.

Climatic modeling

Statistical Downscaling Model (SDSM) Version 4.2 was used to assess site-specific results for changes in atmospheric conditions. This model has been used in various regions of the world and is widely accepted in climate change impact studies (e.g. hydrological modeling). The SDSM is best described as a hybrid of the stochastic weather generator and a regression based on family of transfer function methods (Wilby et al., 2002). It permits the spatial downscaling through daily predictor-predictand relationships using multiple linear regressions, and generates predictands that represent the local weather (Hashmi et al., 2009). The model was calibrated and tested for 12 precipitation stations and five climatic ones. Daily mean temperatures and precipitation sums were downscaled for the period 1970–2080 from the UK Met Office HadCM3 climate model under emissions scenarios SRES A2. The software executes this statistical downscaling of daily weather series through five separate processes: screening of predictor variables, calibration of model, production of observed data (PAR), scenario generation, and statistical analyses.

Data from the Ministry of Water and Irrigation (MWI) (2015) and the Jordan Meteorological Department (JMD) (2014) for stations collected since their respective starting dates were used. Preliminary analysis such as missing values, outliers, and double-mass curves were applied before the more formal time series analysis. Time series analysis includes the application of trend analysis methods and climatic analysis.

Precipitation time series are analyzed for linear trends on a monthly and annual basis. Figure 9 shows the time series for the annual precipitation for selected stations from 1970–2014. There is a slight decreasing trend in the annual precipitation as proposed by the negative slope of the regression line.

All observed data indicate a reduction in the annual precipitation range from approximately 10 to 20%. There have been local reductions in precipitation since the 1970s; however, trends in daily precipitation indices for

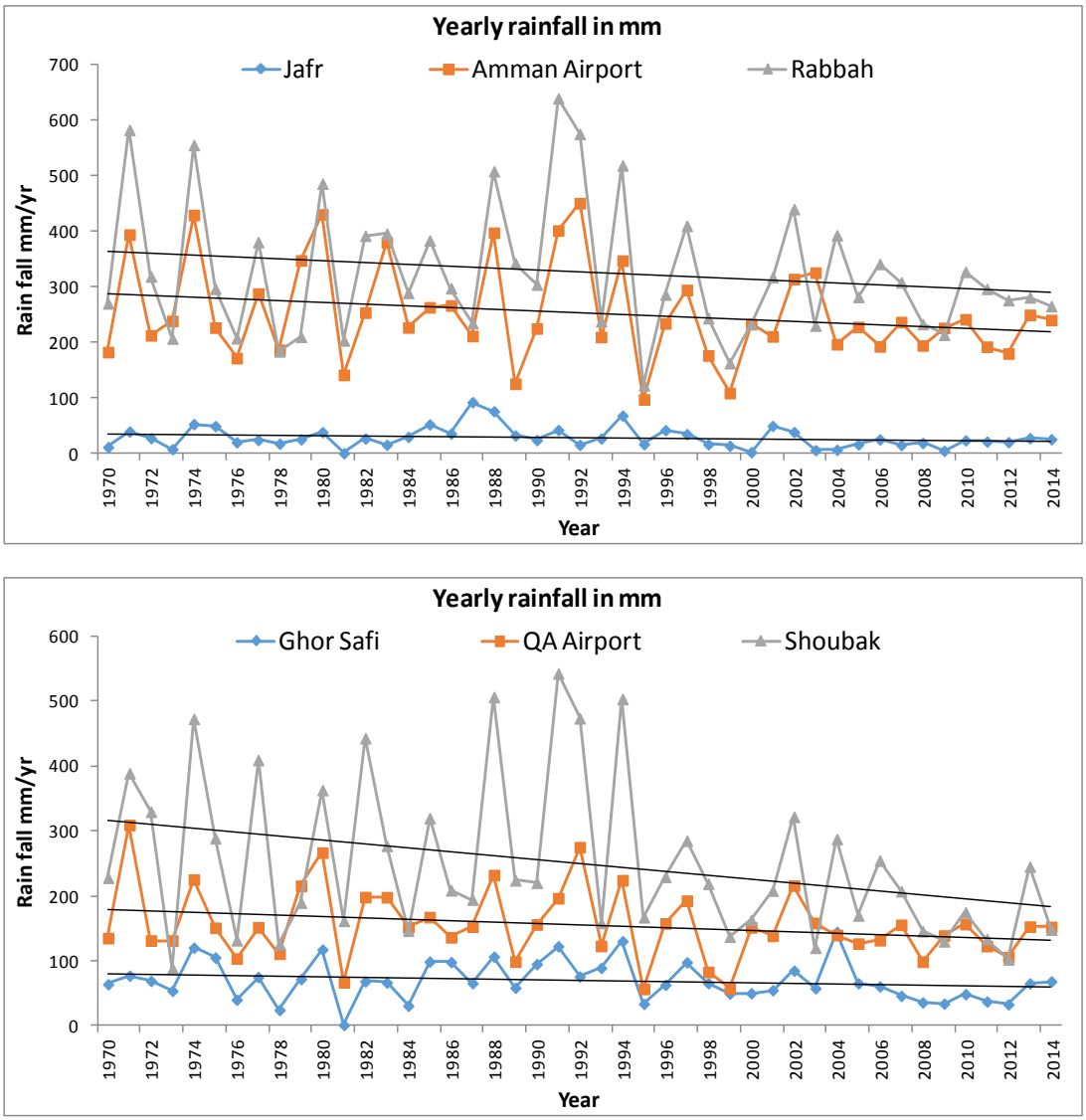

Figure 9. Time series data for annual measured precipitation for selected stations.

Jordan, including the number of rainy days, average intensity of precipitation, and total of maximum daily precipitation—are generally weak and do not show spatial coherence (Zhang et al., 2005).

The data period of the calibrated model spans from 1970-1990 and the validation period from 1991-2010. Figure 10 shows the calibration results between observed stations' variables and modeled values for maximum and minimum temperature as well as for precipitation. Parameters established during the calibration process (that explain the statistical agreement between observed and simulated data) were used for model validation. 10 years data (1991-2014) was used to validate the performance of the model.

The main climatic features which we inspected in the area of study are temperature and precipitation. Five climatic stations were used to investigate future climate scenarios in Mujib Basin. Maximum temperature, minimum temperature, and precipitation time series for the period 1970–2014 were analyzed. The baseline scenarios of the observed climatic parameters were developed using the NCEP Reanalysis data, the Hadley General Circulation Model (HadCM3), and the Statistical Downscaling Model (SDSM).

The Scenario Generator process produces ensembles of synthetic daily maximum and minimum temperature and precipitation at the selected stations of the study area using GCM predictor variables. Regression-based downscaling technique was used to downscale the HadCM3 GCM predictions (Wilby et al., 2002).

Based on the downscaling model; precipitation and temperature for the time period 2015-2080 were predicted

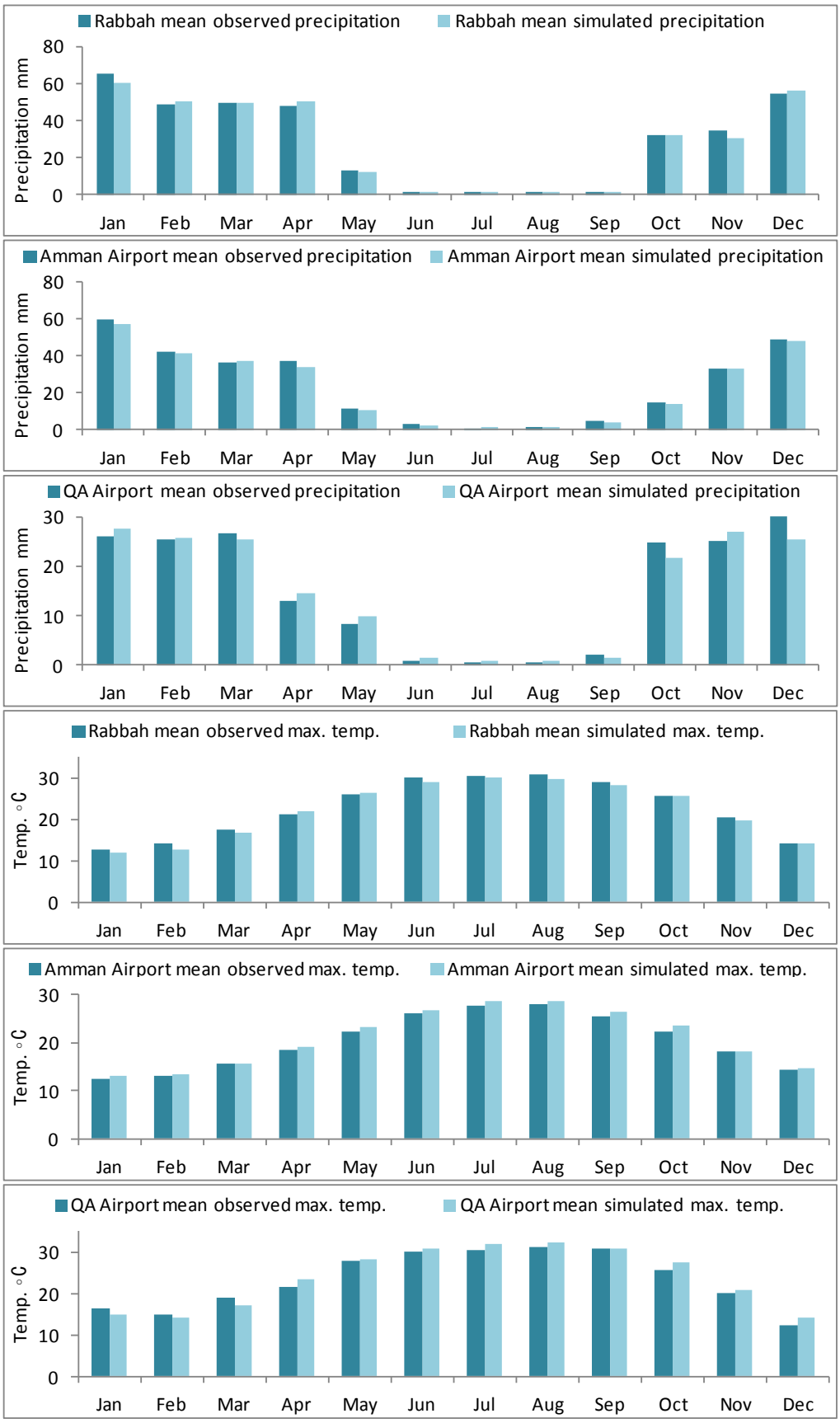

Figure 10. Calibration results for precipitation and temperature downscaling.

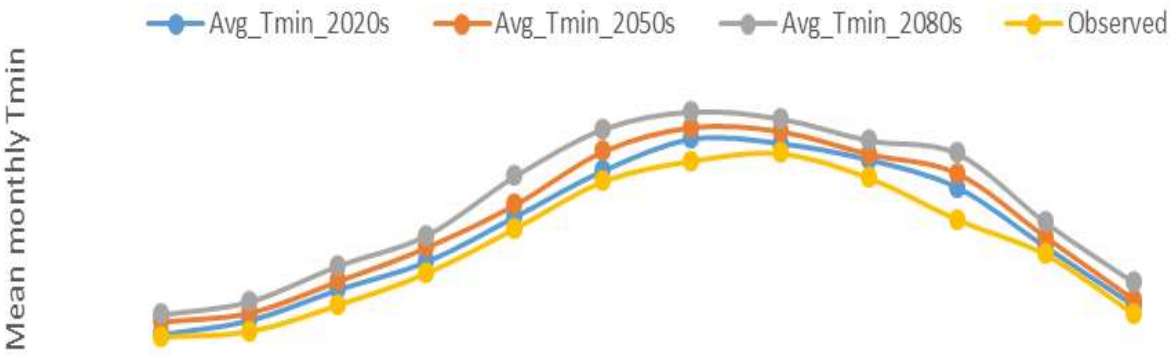

Figure 11. Mean monthly minimum temperature projection for central part of the study area.

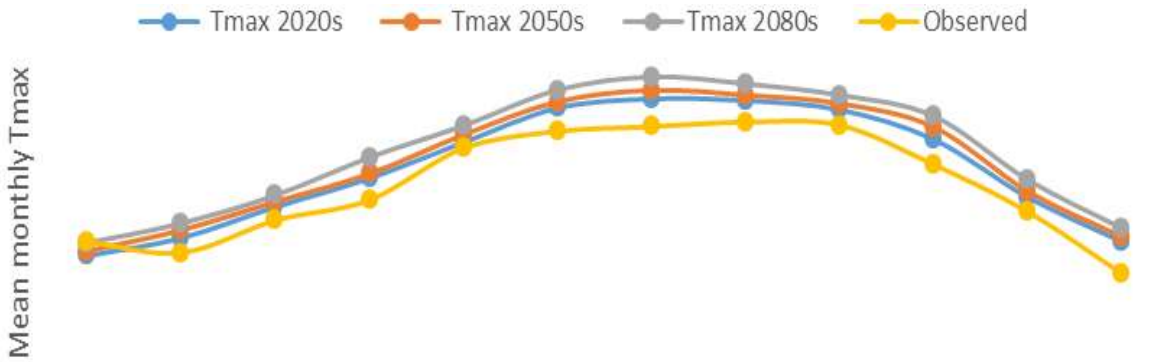

Figure 12. Mean monthly maximum temperature projection for central part of the study area.

on monthly and yearly bases. Figure 11 shows the projection of the monthly mean maximum temperature for the decade periods 2020s, 2050s, and 2080s.

As shown in the figures, most months show an increase in the maximum temperature while the rest show an equal temperature. None of the months show a decrease trend under any scenario. The percentage temperature increase ranges from less than 5 to about 12% in the 2020s, while the potential increase in the maximum temperature ranges from 5 to about 35% in the 2080s. December shows the highest increase over all periods. The model showed that temperature will increase 1.2 and 1.4°C in February and December respectively, while in the 2080s it will hit 4.5 and 4.2°C for the same months.

Figure 12 shows the projection of monthly mean minimum temperature for the 2020s, 2050s, and 2080s. All months shows an increase in the minimum temperature with a potential increase in the minimum temperature ranges from 10 to 33% in the 2050s and 2080s respectively. March and December will have the highest difference in temperature for both the 2020s and the 2050s, whereas in 2080s January and February will display the highest difference in minimum temperature.

Precipitation prediction indicated a dramatic decline as generated from the model, indicating more hydrological cycle disturbance. Precipitation variation was modeled and validated using historical measurements back to 1970 already showing a 9% decline. For the 2020s, 2050s, and 2080s monthly precipitation is shown in Figure 13. The prediction showed that the wettest months of November to March will have the highest vulnerability.

From the models, the highest precipitation reduction will take place in March with 2, 12, and 22% for the years 2020, 2050, and 2080. Predicted yearly precipitation in Mujib Basin for the period 2014–2080 indicated a 21% reduction in precipitation by the year 2080 as shown in Figure 14.

Outputs of the downscaling methods were used to investigate the groundwater recharge's future variation. We used the expected temperature and precipitation for the 2020s, 2050s, and 2080 as inputs to the J2000 model. Based on the predicted temperature and precipitation, water budget components were recalculated in the J2000 focusing on recharge.

Evapotranspiration is expected to drop to 10 to 30% by the year 2080, assuming consistency in current land cover and soil types. Groundwater recharge decreased dramatically by 10, 30, and 70% in the 2020s, 2050s, and

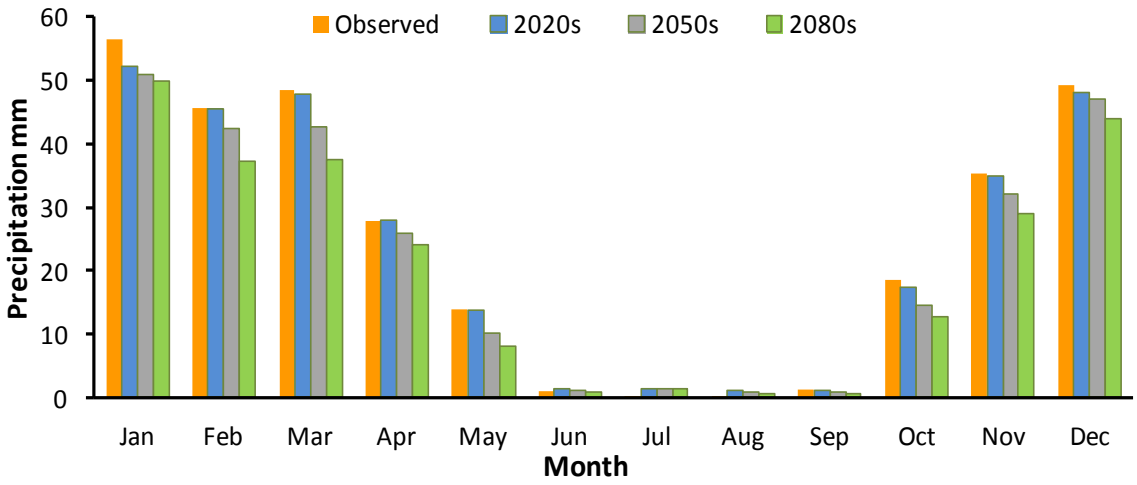

Figure 13. Average monthly precipitation for different periods.

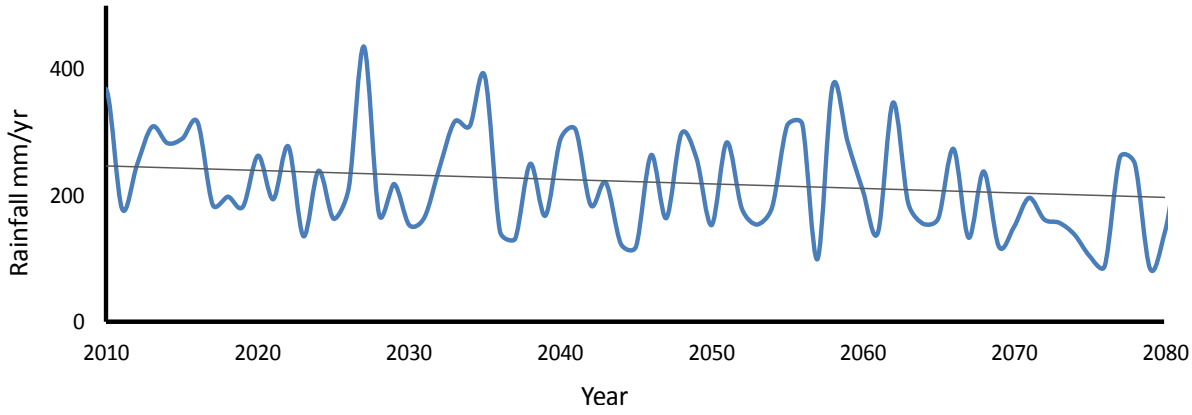

Figure 14. Predicted yearly precipitation in the central part of the area (mm/yr) for the period 2014 – 2080.

2080s respectively from the observed recharge in 2014 as shown in Figure 15. The reduction in recharge rates while keeping pumping at the current levels will cause a drop in water levels, accordingly, the groundwater system will degrade affecting system resilience.

The drop in water level may cause a decline in the saturation thickness and hence transmissivity will be declined as it is a factor of saturated thickness and permeability. According to USGS 2013, the saturated thickness is expected to decline 30 to 70% by the year 2030, accordingly, transmissivity was recalculated for the year 2050 to be in the range of 2 to 400 m^2/day as shown in Figure 16a.

In order to understand groundwater resilience under climate change, a resilience map for the 2050s was compiled based on predicted changes in the resilience factors. Climate change effects on transmissivity, depth to groundwater and groundwater recharge were added since they are all affected by climate change. Also, other parameters such as lithology, pumping rate, etc., were considered as fixed in the model.

The expected increase in the depth to groundwater will affect groundwater resilience negatively, as depth to groundwater is one of the main components of resilience. Within Mujib Basin, the depth to groundwater was expected to be up to 400 m (Figure 16c).

Recharge was recalculated (based on the predicted precipitation and climatic parameters) to be 30% less in the 2050s than the current recharge as shown in Figure 16b.

The resultant groundwater resilience map for the year 2050 (Figure 17) indicated a severe change in the groundwater regime and hydraulics. Following a drop in water level, most of the central parts of the basin are expected to become semi-dry aquifer zones as a result of the limited remaining saturated thickness available for profitable pumping. This is due to the fact that when saturated thickness is less than 20 m pump installation

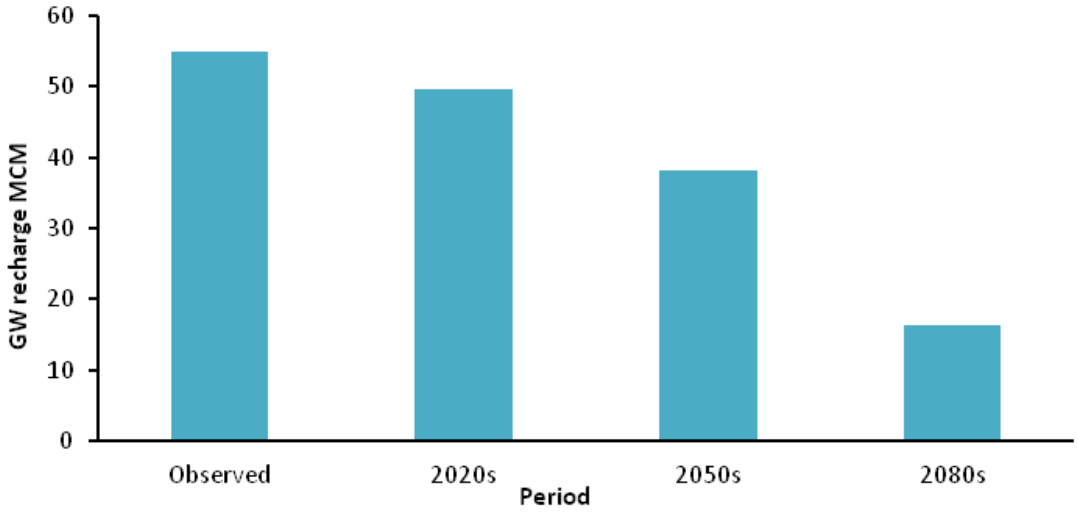

Figure 15. Predicted recharge for the 2020s, 2050s, and 2080s compared to observed in 2014.

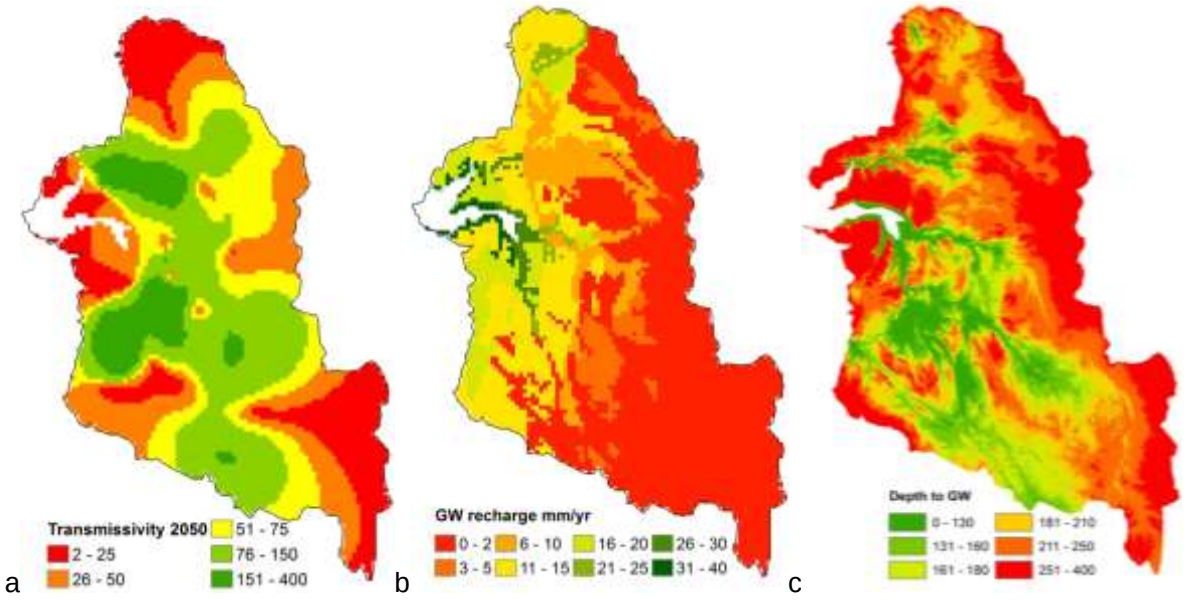

Figure 16. Groundwater resilience parameters affected by climate change (year 2050).

will be risky close to aquifer base. The highest resilience in our model was in the southern parts of the basin due to limited pumping, high transmissivity, and lower climate change impact. Our model predicted that the eastern parts of the basin would be highly affected by climate change, but they displayed moderate resilience due to high transmissivity and specific capacity. High pumping rates and low saturated thickness affected resilience negatively in the central parts of the basin. The expected high impacts in the same areas added more pressures on the system, which shifted from moderate resilience in 2014 to very low in the 2050 s.

DISCUSSION

Our study findings proved that water budget components in the area are under dramatic stress from ongoing climate change forcing and raise the need for urgent action to enhance groundwater resilience to climate change.

Jordan's relatively high population growth of 2.8% (Department of Statistics (DOS), 2010) coupled with refugees influxes add more pressure on vital groundwater basins such as Mujib. With the dependency on groundwater in the country, any deterioration in

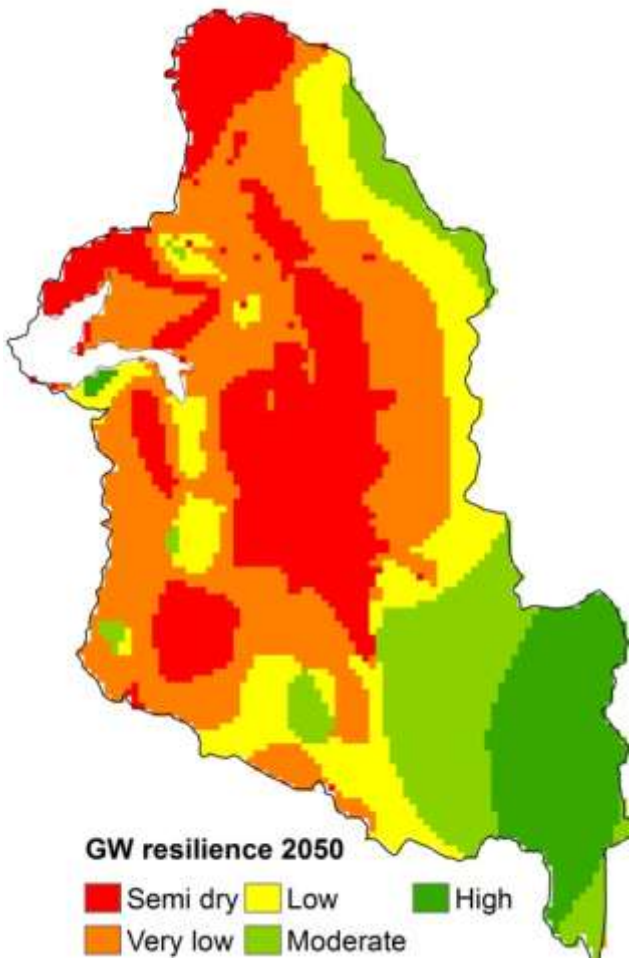

Figure 17. Groundwater resilience map 2050.

resources may lead to highly visible environmental, socio-economic, and health impacts. Groundwater needs to be managed wisely, and resilience of this valuable resource should be considered while defining new well fields.

Jordan's water system is under multiple stresses which are expected to be negatively affected by global warming processes; groundwater resilience is a key factor in influencing groundwater sustainability. Enhancing groundwater resilience will help local communities better adapt to climate change. It also can act to sustain ecosystem services and groundwater supply on different scales.

Studying resilience of groundwater can pave the way for Integrated Water Resources management, a concept that sustains the system under short and long term stresses based on realistic data and hydrological models. The previously-estimated water budget components by GTZ and NRA (1977) and MWI (2003) indicated an underestimation of runoff and overestimation in evapotranspiration as compared to our modeling.

Previous estimates have, however, given a fairly consistent estimate of groundwater recharge with 58 MCM/yr compared to 54 MCM/yr in the current study. The difference in values can be considered realistic, taking into account the recorded 5-7% reduction in precipitation over the last three decades.

Recalculation of the water budget components for Mujib area indicated that recharge to groundwater is limited to 5% of the total yearly precipitation, which lies within the range of total recharge in Jordan of 3-6% (GTZ and NRA, 1977; Schulz, 2013; Wagner, 2011).

Resilience of the groundwater system, as a factor of aquifer hydraulics, lithology, recharge, and abstraction, was found to be very low to high. The most effective component in promoting resilience proved to be the aquifer's saturated thickness, as it plays a vital rule in transmissivity and contributes to the depth of groundwater. Very low resilience areas recorded at the minimum saturated thickness within the central parts of the basin characterized by moderate recharge and over pumping are expected to deteriorate faster than other areas due to continuing climate change.

Climate change impact on resilience is amplified on groundwater recharge due to higher evapotranspiration reducing recharge share and lowered precipitation.

Historical precipitation measurements were used to predict future precipitation until the year 2080, indicating a decline of 21% in the yearly precipitation; this decline coupled with an increase of about 2 to 4°C in temperature will result in groundwater recharge that equals 30% of the current value.

Recharge reduction will cause a dramatic drop in water level, negatively affecting both saturated thickness and depth to groundwater. Such deterioration in the aquifer hydraulics and replenishment rate will decrease the system resilience.

Groundwater resilience for 2050 was modeled as an optimum year for long term planning. Resilience was found to be highly affected in the central part of the basin with 70% less resilience, while areas of high recharge in the west and areas of high saturated thickness and low pumping in the east are expected to have a higher resilience.

Mapping the groundwater resilience in the year 2050 can contribute to the optimum management and sustainability of the groundwater. New well field planning should consider the resilience in order to cope with manmade and natural stresses.

Enhancing resilience in the low and very low classes can be achieved through integrated water resources management. These include distribution of pumping stresses and avoidance of drilling mega well fields, especially in the central parts of the study area.

Enhancement of groundwater recharge is practiced through two main projects in the basin, namely Siwaqa and Wala Dams. Still, areas up stream can be investigated for the Managed Aquifer Recharge (MAR).

Enhancing the resilience will help local communities to adapt to climate change. It also can sustain ecosystem services and groundwater supply on different scales.

Conclusion

The outstanding results of this study has resulted to a groundwater resilience model for Mujib Groundwater Basin. This modified model may help in assessing the current use and pumping practices of groundwater in the study area. It also has a significant value in monitoring the groundwater resilience to continuous climatic variability. Locally, this model can give a future insight of climatic variability effects on one of the most important life assets in Jordan as water shortage is a severe problem that needs managed solutions.

The results indicated that the key players in sustaining groundwater ecosystem and resilience to changes are groundwater recharge and abstraction in relation to the saturation thickness. Here more efforts will be needed to maintain sustainable abstraction and enhance natural recharge through proper land use planning and adaptation of artificial recharge.

Decision makers, researchers and groundwater management interested entities can adopt the proposed model in Jordan's water future plans and policies. Such model sheds the light on the critical sustainability of water resources while the suggested scenarios can aid in the understanding of the different proposed climatic situation with correspondence to the global climatic warming.

CONFLICT OF INTERESTS

The authors have not declared any conflict of interests.

REFERENCES

Abu-Allaban M, El-Naqa A, Jaber M, Hammouri N (2015). Water scarcity impact of climate change in semi-arid regions: A case study in Mujib Basin, Jordan. Arab. J. Geosci. 8(2):951-959.

Aller L, Bennett T, Lehr JH, Petty RJ, Hackett G (1987). DRASTIC: A standardized system for evaluating ground water pollution potential using hydrogeological settings. U.S. Environmental Protection Agency Report, EPA/600/2-87/036, 622p.

Alraggad MM (2009). GIS-based groundwater flow modeling and hydrogeochemical assessment of the northern part of the Dead Sea Groundwater Basin (Doctoral dissertation, PhD. Thesis, University of Jordan, Amman).

BGR (Federal Institute for Geosciences and Natural Resources) and MWI (Ministry of Water and Irrigation)(2005). Groundwater resources of Northern Jordan. Contributions to the hydrology of Northern Jordan. MWI and BGR, Project No. 89.2105.8. Amman, Jordan Vol. 4 (Unpublished).

BGR (Federal Institute for Geosciences and Natural Resources) and WAJ (Water Authority of Jordan) (1995). Groundwater resources of Northern Jordan: Monitoring of groundwater levels in Jordan. WAJ and BGR, BGR-Archive No. 112708, Amman, Jordan Vol. 2, Part 2 (Unpublished).

BGR (Federal Institute for Geosciences and Natural Resources) and WAJ (Water Authority of Jordan) (1996). Groundwater resources of Northern Jordan: Spring discharge in Jordan. WAJ and BGR, BGR-Archive No. 112708, Amman, Jordan Vol. 1, Part 2 (Unpublished).

Department of Statistics (DOS) (2010). Jordan in Numbers. Amman, Jordan.

El-Naser H, Nuseibeh MF, Assaf KK, Kessler S, Ben-Zvi M (1998). Overview of Middle East water resources: water resources of Palestinian, Jordanian, and Israeli interest. http://oregondigital.org/catalog/oregondigital:df70rp65s#page/27/mode/1up

Food and Agriculture Organization (FAO) (1998). Crop evapotranspiration – Guidelines for computing crop water requirements – FAO Irrigation and drainage paper 56, ISBN 92-5-104219-5.

GTZ and NRA (1977). National water master plan of Jordan. Agrar – und Hydrtechnik GMBH ESSE. Bundersanstalt fur Geowissenschaeien und Rohstoffe, Hannover.

Gunderson LH (2000). Ecological resilience – in theory and application. Ecology. Evol. Syst. 31:425-439.

Hashmi MZ, Shamseldin AY, Melville BW (2009). Statistical downscaling of precipitation: State-of-the-art and application of odeling multi-model approach for uncertainty assessment. Hydrol. Earth Syst. Sci. Discussions 6(5):6535-6579.

Healy RW (2010). Estimating groundwater recharge. Cambridge University Press. 264p.

Hjelmfelt AT (1991). Investigation of the Curve Number Procedure. J Hydraul. Eng. ASCE 117:725-737.

Jordan Meteorological Department (JMD) (2014).

Khadeer K (1997). An assessment of regional hydrogeological frame work of the Mesozoic aquifer system of Jordan, PhD research, UK.

Kralisch S, Krause P, Fink M, Fischer C, Flügel WA (2007). Component based environmental modelling using the JAMS framework. In MODSIM 2007 International Congress on Modelling and Simulation pp. 812-818.

Krause P (2002). Quantifying the impact of land use changes on the water balance of large catchments using the J2000 model. Phys. Chem. Earth 27:663-673.

Krause P, Kralisch S (2005). JAMS-The hydrological modeling system J2000—knowledge core for JAMS. In: Proceedings of MODSIM 2005-International Congress on Modelling and Simulation. pp. 676-682.

Kruseman GP, de Ridder NA (1991). Analysis and evaluation of pumping test data. International Institute for Land Reclamation and Improvement, Wageningen. The Netherlands, ISBN 90-70754-207, 377p.

MacDonald AM, Bonsor HC, Calow RC, Taylor RG, Lapworth DJ, Maurice L, Tucker J, Dochartaigh BEO (2011). Groundwater resilience to climate change in Africa. British Geological Survey, 32p. (Unpublished).

Margane A, Hobler M, Almomani M, Subah A (2002). Contributions to the groundwater resources of Northern and Central Jordan Jordan. Geol. Jb., C, 68, 52.

Ministry of Agriculture (MOA) (1993). National soil map and land use project - The soils of Jordan. Hunting Technical Services Ltd. In association with Soil Survey and Land Research Center, Vol. 2.

Ministry of Agriculture (MOA) (1995a). National soil map and land use project - The soils of Jordan. Hunting Technical Services Ltd. In association with Soil Survey and Land Research Center, Vol. 3.

Ministry of Agriculture (MOA) (1995b). National soil map and land use project - The soils of Jordan. Hunting Technical services Ltd. In association with Soil Survey and Land Research Center, Vol. 2 Level 1.

Ministry of Water and Irrigation (MWI) (1993). Water Information System. Hydrological, geological and hydrogeological data bank. MWI, Water Resources and Planning Directorate, Amman, Jordan.

Ministry of Water and Irrigation (MWI) (2014). Jordan Institute for Standards and Metrology: Irrigation Water Quality Guidelines JS. 1st Edition. (In Arabic)

Ministry of Water and Irrigation (MWI) (2015). Open files, Amman.

Ministry of Water and Irrigation (MWI) (2013). Jordan water facts, Amman.

Ministry of Water and Irrigation (MWI) (1995). Jordan water facts, Amman.

Ministry of Water and Irrigation (MWI) (1970). Groundwate hydraulics in central Jordan. MWI, Water Resources and Planning Directorate, Amman, Jordan.
Salameh E (1996). Water Quality Degradation in Jordan (Impact on Environment Economy and Future Generations Resources Base), Friedrich Ebert Stiftung and Royal Society for the Conservation of Nature.
Scheffer F, Schachtschabel P (1984). Iiehrbuch der Bocienkunde. 1a Ed., Ferdinand EnkeVerlag, Stuttgart pp. 271-276.
Schulz S (2013). Application of the water balance model J2000 to estimate groundwater recharge in a semi-arid environment: a case study in the Zarqa River catchment, NW-Jordan. Environ. Earth Sci. 69.2:605-615.
Soil Conservation Service (SCS) (1985). United States Department of Agriculture National Engineering Handbook. Section 4, Hydrology. Washington, DC.
Soil Conservation Service (SCS) (2004). United States Department of Agriculture National Engineering Handbook. Section 4, Hydrology. Washington, DC.
Simsek C (2007). The GIS-integrated surficial aquifer potential mapping and its importance for aquifer protection, Kucuk Menderes Basin/West Turkey. State Hydraulic Works. International Congress on River Basin Management. Vol. 2224.
Solomon S, Qin D, Manning M, Chen Z, Marquis M, Averyt KB, Tignor M, Miller HL (2007). Technical Summary in Climate Change: The Physical Science Basis. Contribution of Working Group I to the Fourth Assessment Report of the Intergovernmental Panel on Climate Change.
United States Geological Survey (USGS) (2013).
Wagner W (2011). Groundwater in the Arab Middle East. Springer, London.
Wilby Robert L, Christian W, Dawson, Elaine M Barrow (2002). SDSM-a decision support tool for the assessment of regional climate change impacts. Environ. Model. Softw. 17.2:145-157.
Wilby RL, Dawson CW, Barrow EM (2002). SDSM - A decision support tool for the assessment of regional climate change impacts. Environ. Model. Softw. 17(2):145-157.
Zhang X, Aguilar E, Sensoy S, Melkonyan H, Tagiyeva U, Ahmed N, Albert P (2005). Trends in Middle East climate extreme indices from 1950 to 2003. J. Geophys. Res. Atmos. P 110.